Progress In Electromagnetics Research B, Vol. 74, 77–91, 2017

Mathematical Model of Large Rectenna Arrays for Wireless Energy Transfer

Dmitriy V. Gretskih[1], Andrey V. Gomozov[2], Victor A. Katrich[3], Anatoliy I. Luchaninov[1], Mikhail V. Nesterenko[3, *], and Yuriy M. Penkin[3]

Abstract—A mathematical model of a large rectenna array (LRA) is presented. It is shown that matrices describing the LRA linear subsystem have a number of specific features that must be considered when the rectenna mathematical model is developed. The state equation for the LRA was obtained. It is shown that the model functioning in nonlinear mode of the infinite rectenna array can be reduced to the parameters of one equivalent receiver-rectifier element (RRE) at the fundamental frequency and its harmonic. The external parameters of RREs and characteristics of LRAs were obtained.

1. INTRODUCTION

Rectennas (rectifying antennas) are part of a wireless power transmission (WPT) system that is intended for receiving microwave energy and converting it into DC power. The rectenna applications open up new possibilities for the solution of actual problems related to the development of innovative technologies for creating highly efficient WPT systems. At present time, the intensive researches are carried out in several areas, including problems associated with the use of solar energy. It is believed that the energy generated by space solar power stations can be transmitted by microwave beams to ground rectenna systems where it will be converted to DC [1–4]. The power supply to consumers of space solar power station in the nearest future is also discussed. The issues concerning rectenna application in the WPT systems for hard-to-reach regions of the Earth [5, 6] and for pilotless aerial vehicles systems [4, 7] are extensively investigated. Relatively new areas of wireless power engineering are related to energy harvesting from the background electromagnetic fields [8, 9] and to transformation of the optical radiation into DC power by using nanorectennas [10].

Efficiency of the WPT system is largely determined by its terminal device, i.e., rectenna, which is a non-phased array of the RREs consisting of receiving antenna and rectifier circuits. Depending on the load power, the rectenna arrays may be small or large and include from a few up to 10^6 of RREs. Main RRE parameters include several quality indicators, namely: the coefficient of performance (COP) of the rectenna conversion, reradiation levels at upper harmonic, reliability, cost and suitability for mass production. For the LRAs used in high-power WPT systems, questions concerning the optimization of the individual RRE parameters and characteristics of the entire rectenna array as a whole are actual today along with the problem of improving the parameters of the individual rectifier diodes. Of course, this optimization can be realized only by mathematical modeling. However, mathematical models developed earlier and analysis of the rectenna based on these models have very limited applications. These limitations are manifested in two ways: 1) the models are simplified very much; the radiators have the simplest configuration [11]; the mutual influence of array elements was not taken into account;

Received 5 January 2017, Accepted 23 March 2017, Scheduled 10 April 2017

* Corresponding author: Mikhail V. Nesterenko (mikhail.v.nesterenko@gmail.com).
[1] Kharkov National University of Radio Electronics, 14, Nauki Ave., Kharkov 61166, Ukraine. [2] Certification Center of Space-Rocket Technique Kharkov Representative Office of the General Customer, State Space Agency of Ukraine, 271, Academic Pavlov str., Kharkov 61054, Ukraine. [3] V. N. Karazin Kharkov National University, 4, Svobody Sq., Kharkov 61022, Ukraine.

2) the models are universal, but they do not adequately reflect all processes associated with the presence of nonlinear elements (NEs) [12]. In addition, some models can be used only for studying of single RRE and small rectenna arrays [13, 14]. Therefore, the development of new efficient LRA models is a very practical problem.

This paper is devoted to the development of a rectenna mathematical model suitable for the analysis of periodic excitation mode for a sufficiently broad class of single rectenna elements taking into account nonlinear processes and for the LRA built on their basis. The model combines the multipole theory and rigorous electrodynamic analysis of antenna array elements.

2. MATHEMATICAL MODEL OF LARGE RECTENNA ARRAYS

2.1. Problem Formulation

Since the rectenna array (Fig. 1) contains nonlinear elements, the rectifier diodes, nonlinear effects of the rectenna parameters upon the level of the input stimulus, and formation of new spectral components in the rectenna response can be manifested. The nonlinear effects depend upon the rectenna schematic and radiator design parameters, linear and nonlinear elements included in the rectenna circuit. Therefore, the correct analysis of the LRA should include the inherent nonlinear effects requiring a complex approach, which takes into account the characteristics of the nonlinear circuit and radiators, interrelation between them and the DC power collection circuit. In other words, the rectenna should be considered as single complex device with nonlinear characteristics.

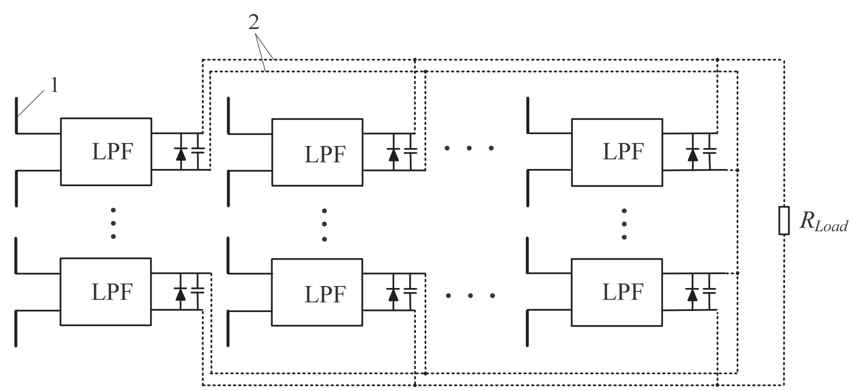

Figure 1. The rectenna array schematics: 1 — radiator; 2 — wires of the power collection circuit; LPF — low-pass filter.

To construct the mathematical model of the rectenna system, it is appropriate to carry out its conditional decomposition on a number of separate components characterized by a matrix of parameters. In this case, the model universality will be provided by an autonomous analysis of separate components. Therefore, a necessary step in building the general rectenna model should include a preliminary description of its individual component based on a general method of antenna analysis [15–17].

Let us consider a planar array consisting of identical RREs placed in nodes of the oblique grid with double periodicity along axes x and l (Fig. 2). The periods along the axes x and l are equal to d_x and d_l, respectively. The angle between axes x and l is equal to α_r. A cell with indices $(0, 0)$ is called the central cell. The position of each RRE is defined by the indices (p, q) which correspond to the point with radius vector $\rho_{pq} = pd_x\mathbf{x}_0 + qd_l\mathbf{l}_0$. Here $\mathbf{x}_0$, $\mathbf{l}_0$ are the unit vectors in the directions x and l.

The rectenna array is irradiated by a plane electromagnetic wave coming from the direction θ, φ (Fig. 2). The wave angular frequency is ω_0, and the wavelength in free space is λ. The electric field vector of the irradiating wave in an arbitrary point with coordinates (x, y, z) can be written as

$$\mathbf{E}(x, y, z) = \mathbf{E}_0 \exp\left[jk_0\left(x \sin\theta \cos\varphi + y \sin\theta \sin\varphi + z \cos\theta\right)\right], \tag{1}$$

where $k_0 = 2\pi/\lambda_0$, $\mathbf{E}_0$ is the wave amplitude.

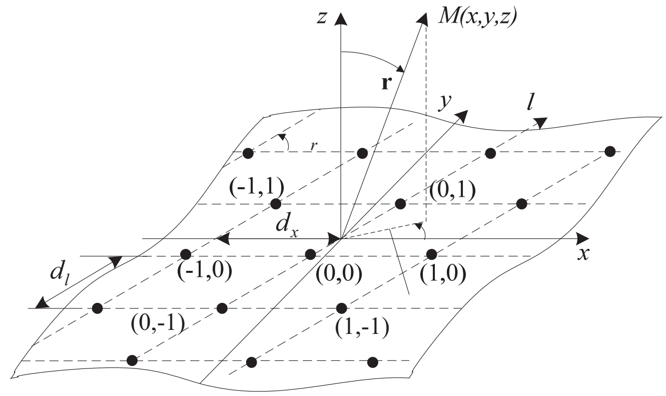

Figure 2. The periodic structure of the rectenna array.

2.2. Large Rectenna Array Schematic

A general block diagram, which allows us to describe various rectenna arrays, is shown in Fig. 3 where common linear subcircuits, LS-1 and LS-2, are separated out in the rectenna. The subcircuit LS-1 corresponds to the radiator system, and the subcircuit LS-2 relates to the power collection and load circuits. In addition, linear LS-3 and nonlinear subcircuits (NS) combine all linear and nonlinear elements of each RRE.

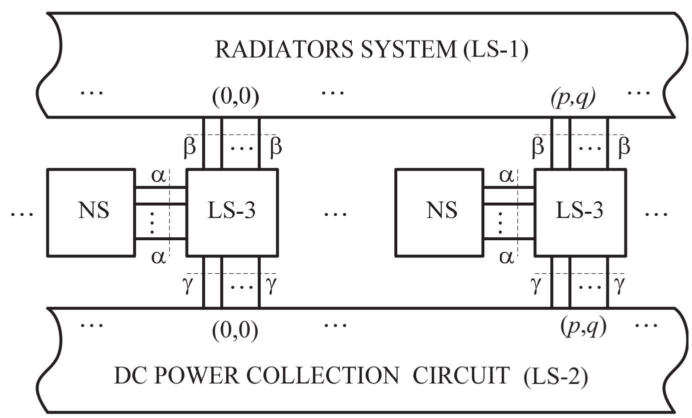

Figure 3. The block-diagram of the rectenna array.

The division of the block-diagram into subcircuits is determined by several factors, of which the following should be considered. Firstly, in many cases, the rectenna models of different complexity levels may be required depending on analysis depth and the accuracy of results. Secondly, the characteristics of rectenna linear and nonlinear elements differ quite substantially.

The element NS will be presented as a nonlinear 2-N_α-multipole (NM) (Fig. 4(a)), described by the mapping $\Re$, which maps its input voltage vector $\mathbf{u}_{nl}(t) = (u_{nl1}(t), u_{nl2}(t), \ldots, u_{nlN_\alpha}(t))^T$ on the current vector $\mathbf{i}_{nl}(t) = (i_{nl1}(t), i_{nl2}(t), \ldots, i_{nlN_\alpha}(t))^T$, i.e.,

$$\mathbf{i}_{nl}(t) = \Re\{\mathbf{u}_{nl}(t)\} \tag{2a}$$

or vice versa

$$\mathbf{u}_{nl}(t) = \Re^{-1}\{\mathbf{i}_{nl}(t)\}. \tag{2b}$$

Here N_α is the number of inputs, which connect the NM with multipole corresponding to subcircuit LS-3 (cross-section α-α); superscript T denotes transposition. For each linear subcircuit, we set a one-to-one

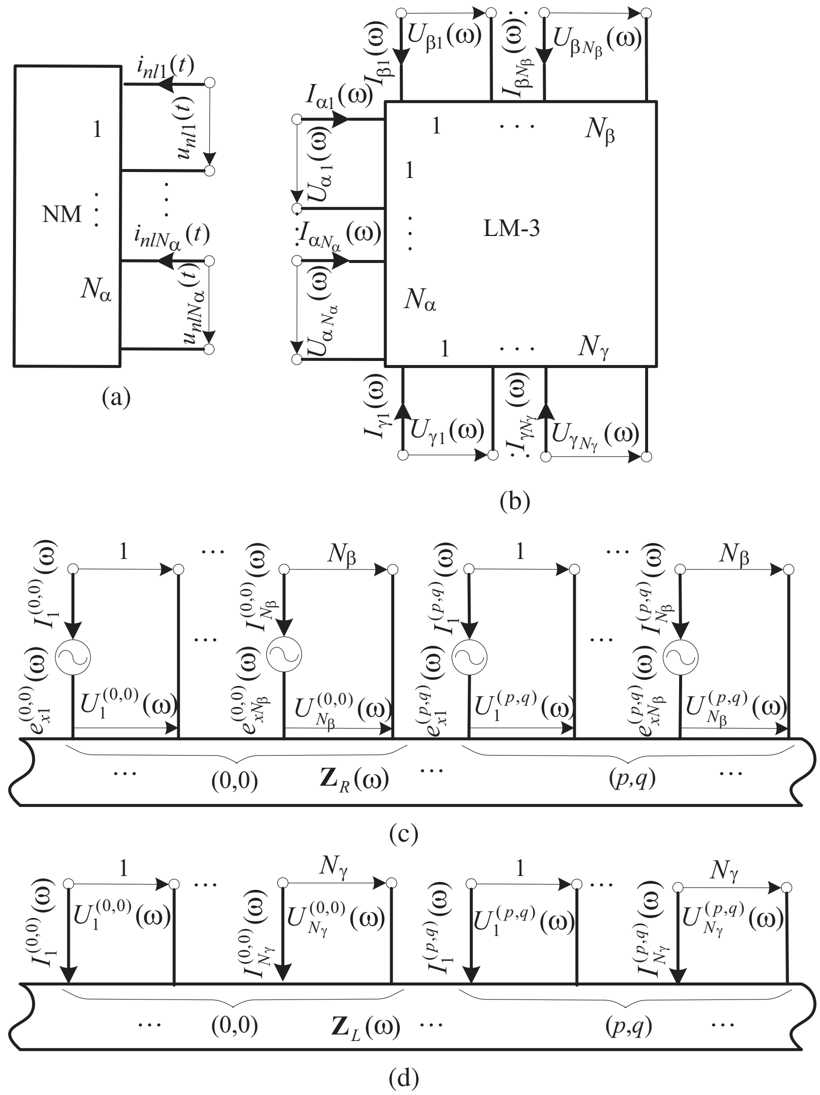

Figure 4. The rectenna subcircuits as multipole at the step of determining the state variables.

correspondence between the linear multipoles LM-1, LM-2 and LM-3 (Figs. 4(b), (c), (d)). Unlike the NM, linear multipoles can be described more conveniently in the frequency domain.

Before choosing system parameters describing the linear rectenna multipoles, we will note the following. The procedure of the rectenna analysis can be divided into several stages. This division, as well as the content of the individual steps is to some extent arbitrary. It depends upon the approach used for the analysis. However, any approach should include a stage of the operating mode selection for the analyzed device and a stage of determining its external parameters. These stages for the LRA analysis are as follows.

At the first stage, according to an infinite array approximation, which will be used below, we assume that the operating mode of each RRE corresponds to that of the element included into an infinite array. Therefore, the infinite array of the RRE ($N_x, N_l \to \infty$) should be considered on the first step, and hence, the multipoles LM-1, LM-2 have infinite number of inputs. The parameters define the linear multipoles from the inputs, which are connected with each other, i.e., relative to the cross-sections α-α, β-β and γ-γ.

At the second stage, the external parameters are defined, and the rectenna is considered as an array with a finite number of RRE ($N_x \times N_l$). Consequently, the multipoles LM-1 and LM-2 should be described by finite dimensional matrices. At this stage, the parameters characterizing the interaction between the radiator system and external medium must be known, i.e., the complete system of parameters describing the LM-1 is also required. Therefore, it is quite natural that the systems of parameters describing linear multipoles can be selected at various stages of analysis. The main criterion, which determines what parameters should be used, is the convenience of their application for specific tasks.

2.3. Analysis of the Nonlinear Regime of the Large Rectenna

Determination of a nonlinear device mode consists in solution of the device state equation [15, 16]. Below we will consider some aspects of such a system formation and its features for the LRA.

2.3.1. Description of Linear Multipoles

To form a system of state equations, the multipole LM-1, characterized by an infinite periodic radiator system, can be conveniently described by using the following data: the angular frequency ω, matrix of self and mutual impedances $\mathbf{Z}_R(\omega)$, and complex amplitudes of the electro-motive force (EMF) $\mathbf{e}_\beta(\omega)$ induced at inputs of radiators by the field of the plane wave (Fig. 4(c)). The matrix $\mathbf{Z}_R(\omega)$ for the flat infinite periodic radiator array excited by the plane wave is the infinite block-block-Toeplitz (BBT) matrix, and the external stimulus on the radiator inputs can be represented by the EMF source system with a double periodicity. This can be explained as follows. If the external excitation is described by Equation (1), the field intensity of the plane wave in point M_{00} belonging to the central cell and the field intensity at the point M_{pq} are related as

$$\mathbf{E}\left(M_{p,q}\right) = \mathbf{E}\left(M_{0,0}\right) \exp\left[j\left(ap + bq\right)\right], \tag{3}$$

where $a = k_0 d_x \sin\theta\cos\varphi$, $b = k_0 d_l (\sin\theta\cos\varphi\cos\alpha_r + \sin\theta\sin\varphi\sin\alpha_r)$. Therefore, the amplitudes of EMF induced by the field of the plane wave at the radiators inputs, located in the cells $(0, 0)$ and (p, q) which are converted to the cross-sections β-β (Fig. 3), are related as

$$\mathbf{e}_\beta^{(p,q)}\left(\omega_0\right) = \mathbf{e}_\beta^{(0,0)}\left(\omega_0\right) \exp\left[j\left(ap + bq\right)\right]. \tag{4}$$

Here $\mathbf{e}_\beta^{(p,q)}(\omega_0)$ and $\mathbf{e}_\beta^{(0,0)}(\omega_0)$ are the complex amplitude of the radiators EMF arranged in periodic nodes with indices (p, q) and $(0, 0)$, respectively. This relationship describes the system of EMF sources with the double periodicity.

The multipole LM-2 (Fig. 4(d)) has an infinite number of inputs and is described by the impedance matrix $\mathbf{Z}_L(\omega)$, which relates the complex current amplitudes $\mathbf{I}(\omega)$ and the voltages $\mathbf{U}(\omega)$ at its inputs (cross-section γ-γ) as

$$\mathbf{U}\left(\omega\right) = \mathbf{Z}_L\left(\omega\right)\mathbf{I}\left(\omega\right). \tag{5}$$

Here the vectors $\mathbf{I}(\omega)$ and $\mathbf{U}(\omega)$ are formed as follows

$$\begin{aligned}\mathbf{I}\left(\omega\right) &= \left(\ldots, I_1^{(-1,0)}, I_2^{(-1,0)}, \ldots, I_{N_\gamma}^{(-1,0)}, I_1^{(0,0)}, I_2^{(0,0)}, \ldots, I_{N_\gamma}^{(0,0)}, I_1^{(1,0)}, I_2^{(1,0)}, \ldots, I_{N_\gamma}^{(1,0)}, \ldots\right)^T, \\ \mathbf{U}\left(\omega\right) &= \left(\ldots, U_1^{(-1,0)}, U_2^{(-1,0)}, \ldots, U_{N_\gamma}^{(-1,0)}, U_1^{(0,0)}, U_2^{(0,0)}, \ldots, U_{N_\gamma}^{(0,0)}, U_1^{(1,0)}, \ldots, U_{N_\gamma}^{(1,0)}, \ldots\right)^T.\end{aligned}$$

Let us assume that all RRE are loaded by identical resistors. The multipole LM-3 (Fig. 4(b)), corresponding to subcircuit LS-3 can be described by the impedance matrix which relates the complex amplitudes of the currents and voltages in the cross-sections α-α, β-β, and γ-γ. This relationship can be written in block form as

$$\begin{pmatrix} \mathbf{U}_\alpha(\omega) \\ \mathbf{U}_\beta(\omega) \\ \mathbf{U}_\gamma(\omega) \end{pmatrix} = \begin{pmatrix} \mathbf{Z}'_{\alpha\alpha}(\omega) & \mathbf{Z}'_{\alpha\beta}(\omega) & \mathbf{Z}'_{\alpha\gamma}(\omega) \\ \mathbf{Z}'_{\beta\alpha}(\omega) & \mathbf{Z}'_{\beta\beta}(\omega) & \mathbf{Z}'_{\beta\gamma}(\omega) \\ \mathbf{Z}'_{\gamma\alpha}(\omega) & \mathbf{Z}'_{\gamma\beta}(\omega) & \mathbf{Z}'_{\gamma\gamma}(\omega) \end{pmatrix} \begin{pmatrix} \mathbf{I}_\alpha(\omega) \\ \mathbf{I}_\beta(\omega) \\ \mathbf{I}_\gamma(\omega) \end{pmatrix}. \tag{6}$$

Here $\mathbf{I}_j(\omega) = (I_{j1}(\omega), I_{j2}(\omega), \ldots, I_{jN_j}(\omega))^T$ and $\mathbf{U}_j(\omega) = (U_{j1}(\omega), U_{j2}(\omega), \ldots, U_{jN_j}(\omega))^T$ are vectors whose elements are the complex amplitudes of the currents and voltages at the terminals of LM-3, which are connected to other multipoles (cross-sections α-α, β-β and γ-γ).

Thus, relations (2)–(6) completely describe all multipoles, which are included in the generalized rectenna circuit and are necessary for the formation of state equations. Then we define the matrix of intrinsic and mutual impedances and the system of the EMF vectors, which describe the entire linear circuit relative to the cross-sections α-α, where they are connected with the nonlinear multipole. These properties allow us to simplify the solution of state equations for the LRA using approximation of the infinite rectenna array.

2.3.2. Properties of the Linear Subcircuit of the Infinite Rectenna Array

Let us transform the linear subcircuit of the rectenna, which includes three linear subcircuits (Fig. 3) in such a way that the linear subcircuit LS-3 is unchanged, while subcircuits LS-1 and LS-2 form a new combined subcircuit coupled to the subcircuit LS-3 in the cross-section σ-σ (Fig. 5).

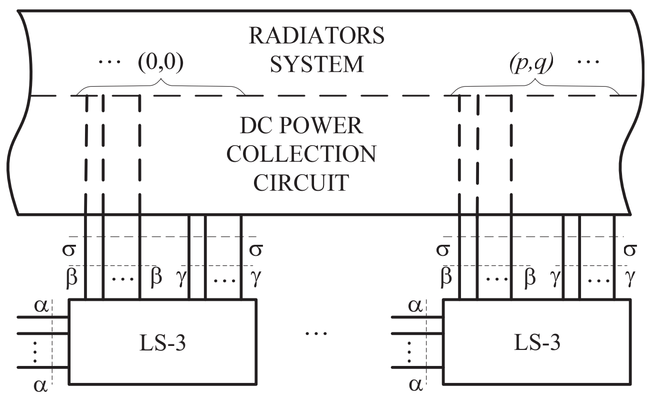

Figure 5. The modified linear subcircuit of the rectenna.

Let $\mathbf{Z}^{\Sigma}(\omega)$ be the matrix of intrinsic and mutual impedances of the combined multipole corresponding to the radiators system and DC power collection circuit with respect to the cross-section σ-σ. Since the matrices of the multipoles LM-1 and LM-2 are block-block-Toeplitz (BBT) matrices, matrix $\mathbf{Z}^{\Sigma}(\omega)$ has the same properties by virtue of the assumption concerning the identical RRE loads.

The matrices of the multiports LM-3 can be presented in the block form

$$\mathbf{Z}(\omega) = \begin{pmatrix} \mathbf{Z}'_{\alpha\alpha}(\omega) & \mathbf{Z}'_{\alpha\sigma}(\omega) \\ \mathbf{Z}'_{\sigma\alpha}(\omega) & \mathbf{Z}'_{\sigma\sigma}(\omega) \end{pmatrix}, \tag{7}$$

where $\mathbf{Z}'_{ij}(\omega)$ are the blocks describing the interaction between the inputs belonging to the cross-sections i, and j $(i, j = \alpha, \sigma)$. Taking into account the accepted notation, the matrix of intrinsic and mutual impedances $\mathbf{Z}_{\alpha\alpha}(\omega)$ relative to the inputs connected to the nonlinear multipoles (Fig. 5) and the complex EMF amplitudes $\mathbf{e}_x(\omega)$ on the same inputs can be determined from the relations

$$\begin{aligned} \mathbf{Z}_{\alpha\alpha}(\omega) &= \mathbf{Z}''_{\alpha\alpha}(\omega) - \mathbf{Z}''_{\alpha\sigma}(\omega)\left(\mathbf{Z}''_{\sigma\sigma}(\omega) + \mathbf{Z}^{\Sigma}(\omega)\right)^{-1}\mathbf{Z}''_{\sigma\alpha}(\omega), \\ \mathbf{e}_x(\omega) &= -\mathbf{Z}''_{\alpha\sigma}(\omega)\left(\mathbf{Z}''_{\sigma\sigma}(\omega) + \mathbf{Z}^{\Sigma}(\omega)\right)^{-1}\mathbf{e}_{x\sigma}(\omega), \end{aligned} \tag{8}$$

where $\mathbf{Z}''_{ij}(\omega)$ are infinite-dimensional block-diagonal matrices. The elements of these matrices are the blocks $\mathbf{Z}'_{ij}(\omega)$ of the matrices $\mathbf{Z}(\omega)$. In Eq. (8), vector $\mathbf{e}_{x\sigma}(\omega)$ is an infinite-dimensional vector formed as follows

$$\begin{aligned} \mathbf{e}_{x\sigma}(\omega) \; = \; \Big(&\ldots, \mathbf{e}_{\beta}^{(-1,-q)}(\omega), \mathbf{0}, \mathbf{e}_{\beta}^{(0,-q)}(\omega), \mathbf{0}, \ldots, \mathbf{e}_{\beta}^{(-1,0)}(\omega), \mathbf{0}, \mathbf{e}_{\beta}^{(0,0)}(\omega), \mathbf{0}, \\ &\ldots, \mathbf{e}_{\beta}^{(-1,q)}(\omega), \mathbf{0}, \mathbf{e}_{\beta}^{(0,q)}(\omega), \mathbf{0}, \ldots\Big)^T. \end{aligned} \tag{9}$$

Here $\mathbf{e}_{\beta}^{(p,q)}(\omega)$ is the vector defined by Eq. (4); $\mathbf{0}$ is the zero vector whose dimension is equal to the number of RRE inputs in the cross-section γ-γ. The presence of the zero vector in Eq. (9) reflects the fact that the multipole LM-2 does not contain independent sources. Since the diagonal blocks of each matrix $\mathbf{Z}''_{ij}(\omega)$ are identical, they are a special case of BBT matrices which, in turn, have the properties of circulant matrices. The circulant matrix with complex entries has the following properties:

- if a circulant matrix is non-singular, then its inverse matrix is also circulant;
- a set of circulant matrices is a commutative ring;
- a set of non-singular circulant matrices is a commutative group under multiplication.

These properties allow us to state that the matrices $\mathbf{Z}_{\alpha\alpha}(\omega)$ and $\mathbf{Z}''_{\alpha\sigma}(\omega)(\mathbf{Z}''_{\sigma\sigma}(\omega)+\mathbf{Z}^{\Sigma}(\omega))^{-1}\mathbf{Z}''_{\sigma\alpha}$ (ω) are BBT matrices, while the infinite-dimensional vector $\mathbf{e}_x(\omega)$ whose elements as well as elements of the vector $\mathbf{e}_x(\omega)$ satisfy relation (4), i.e.,

$$\mathbf{e}_x^{(p,q)}(\omega) = \mathbf{e}_x^{(0,0)}(\omega)\exp\left[j\left(ap+bq\right)\right]. \tag{10}$$

where $\mathbf{e}_x^{(p,q)}(\omega)$ and $\mathbf{e}_x^{(0,0)}(\omega)$ are the EMF complex amplitudes induced by the incident wave at the terminals of the radiating system converted to the cross-sections α-α of the RREs which are placed in cells with numbers (p,q) and $(0,0)$, respectively. Therefore, the EMF vector in the time domain can be written as

$$\mathbf{e}_x^{(p,q)}(t) = \mathbf{e}_x^{(0,0)}\left[t+(a/\omega)\,p+(b/\omega)\,q\right]. \tag{11}$$

We will show how these properties of the linear subcircuit and EMF vector can be used to solve the LRA state equations in the approximation of the infinite RRE array.

2.3.3. LRA State Equations

To derive the state equations, we have the following steps:

a) Let $\mathbf{Z}_{p,q}^{k,l}(\omega)$ be the block of matrix $\mathbf{Z}_{\alpha\alpha}(\omega)$ describing the interaction between groups of inputs, which are connected to the nonlinear multipoles RRE (Fig. 6) related to cells with numbers (p,q) and (k,l); the superscripts and subscripts points to rows and columnd defining a position of the block $\mathbf{Z}_{p,q}^{k,l}(\omega)$ in the matrix;
b) Let us form a matrix sequence $\{\mathbf{Z}_{p,q}\}$ from elements of the zero row ($k=0$, $l=0$) of the matrix $\mathbf{Z}_{\alpha\alpha}(\omega)$ in the following way

$$\begin{aligned}&\{\ldots,\mathbf{Z}_{-1,-q}(\omega),\mathbf{Z}_{0,-q}(\omega),\mathbf{Z}_{1,-q}(\omega),\ldots,\mathbf{Z}_{-1,0}(\omega),\mathbf{Z}_{0,0}(\omega),\mathbf{Z}_{1,0}(\omega),\\&\ldots,\mathbf{Z}_{-1,q}(\omega),\mathbf{Z}_{0,q}(\omega),\ldots,\mathbf{Z}_{1,q}(\omega),\ldots\},\end{aligned} \tag{12}$$

where $\mathbf{Z}_{p,q}(\omega)=\mathbf{Z}_{p,q}^{0,0}(\omega)$;

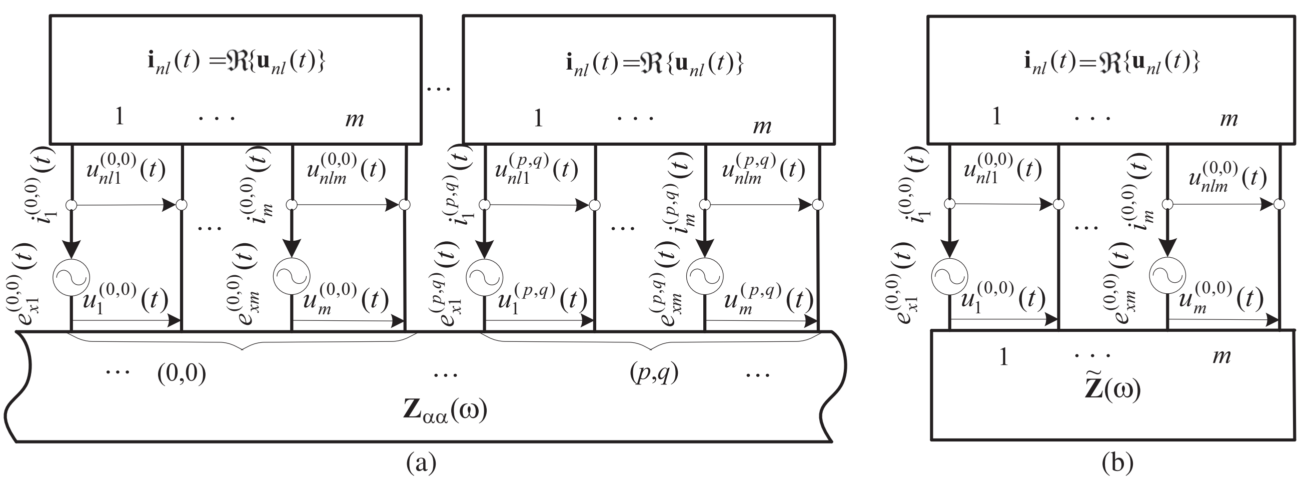

Figure 6. Schematics of the infinite periodic array of the RRE.

c) Let us assume that the nonlinear multiports of the RRE are described by relation (2a) and have $m = N_\alpha$ inputs (Fig. 6(a)).

Now consider the representation of current $\mathbf{i}^{(p,q)}(t)$ and voltage $\mathbf{u}^{(p,q)}(t)$ related to the cell (p,q) which describe the mode of the LS input group and are connected to the nonlinear multipole. The state variables, currents or voltages on the nonlinear elements under the periodic input stimuli can be represented by a Fourier series

$$\mathbf{i}^{(p,q)}(t) = \sum_{n=-\infty}^{\infty} \delta_n \mathbf{I}_n^{(p,q)} \exp(jn\omega_0 t), \tag{13}$$

where $\mathbf{I}_n^{(p,q)}$ is the m-dimensional vector, whose elements are the complex amplitudes of the n-th current harmonics for LS input groups with (p,q) indices (cross-section α-α); $\delta_n = 1$ if $n = 0$ and $\delta_n = 1/2$ if $n \neq 0$. Since the condition in Eq. (11) for the EMF vector is fulfilled, and the matrix of the linear subcircuit is the BBT matrix, then

$$\mathbf{i}^{(p,q)}(t) = \mathbf{i}^{(0,0)}\left[t + (a/\omega_0)\,p + (b/\omega_0)\,q\right]. \tag{14}$$

The relation between the complex amplitudes of the n-th harmonic currents on the LS inputs with the indices (p,q) and zero indices $(0,0)$ can be obtained by comparing formulas (13) and (14)

$$\mathbf{I}_n^{(p,q)} = \mathbf{I}_n^{(0,0)} \exp\left[jn\,(ap + bq)\right]. \tag{15}$$

The time dependence of the voltage at the same LS inputs can be written as

$$\mathbf{u}^{(p,q)}(t) = \sum_{n=-\infty}^{\infty} \delta_n \mathbf{U}_n^{(p,q)} \exp(jn\omega_0 t), \tag{16}$$

where $\mathbf{U}_n^{(p,q)}$ are complex amplitudes of the n-th harmonic on the LS inputs with the indices (p,q). The vectors $\mathbf{U}_n^{(p,q)}$ and $\mathbf{I}_n^{(p,q)}$ are related as

$$\mathbf{U}_n^{(p,q)} = \sum_{k=-\infty}^{\infty} \sum_{l=-\infty}^{\infty} \mathbf{Z}_{k,l}^{p,q}(n\omega_0)\mathbf{I}_n^{(k,l)} = \tilde{\mathbf{Z}}(n\omega_0)\,\mathbf{I}_n^{(p,q)}, \tag{17a}$$

where

$$\begin{aligned}\tilde{\mathbf{Z}}(n\omega_0) &= \sum_{k=-\infty}^{\infty} \sum_{l=-\infty}^{\infty} \mathbf{Z}_{k,l}^{p,q}(n\omega_0) \exp\left\{jn\left[a(k-p) + b(l-q)\right]\right\} \\ &= \sum_{k=-\infty}^{\infty} \sum_{l=-\infty}^{\infty} \mathbf{Z}_{k,l}(n\omega_0) \exp\left\{jn\left[ak + bl\right]\right\}. \end{aligned} \tag{17b}$$

Consequently,

$$\mathbf{u}^{(p,q)}(t) = \sum_{n=-\infty}^{\infty} \delta_n \tilde{\mathbf{Z}}(n\omega_0)\,\mathbf{I}_n^{(p,q)} \exp\{jn\omega_0 t\}. \tag{18}$$

The resulting representation of $\mathbf{i}^{(p,q)}(t)$ and $\mathbf{u}^{(p,q)}(t)$ allows us to write down the system of the state equations for the rectenna as follows

$$\sum_{n=-\infty}^{\infty} \delta_n \mathbf{I}_n^{(p,q)} \exp\{jn\omega_0 t\} + \Re\left\{\sum_{n=-\infty}^{\infty} \delta_n \tilde{\mathbf{Z}}(n\omega_0)\,\mathbf{I}_n^{(p,q)} \exp\{jn\omega_0 t\} + \mathbf{e}^{(p,q)}(t)\right\} = 0, \tag{19}$$

for any $p, q \in -\infty, \infty;, t \in [0,T]$. The solutions of this equation system are the amplitudes of the current harmonics $\mathbf{I}_n^{(p,q)}$ for all groups of the LS inputs. All equations of the system are determined for a temporal interval $t \in [0,T]$. Taking into account relations (14), (15), and (16), we can transform the system of equations for the currents at the inputs with the zero indices for any $p, q \in -\infty, \infty$; $t \in [0, T]$ to

$$\sum_{n=-\infty}^{\infty} \delta_n \mathbf{I}_n^{(0,0)} \exp\{jn\omega_0 [t + (a/\omega_0) p + (b/\omega_0) q]\}$$
$$+\Re\left\{ \sum_{n=-\infty}^{\infty} \delta_n \tilde{\mathbf{Z}} (n\omega_0) \mathbf{I}_n^{(0,0)} \exp\{jn\omega_0 [t + (a/\omega_0) p + (b/\omega_0) q]\} \right.$$
$$\left. + \mathbf{e}^{(0,0)} [t + (a/\omega_0) p + (b/\omega_0) q] \right\} = 0 \tag{20}$$

for any $p, q \in -\infty, \infty$; $t \in [\Delta t^{(p,q)}, T + \Delta t^{(p,q)}]$, where $\Delta t^{(p,q)} = (a/\omega_0)p + (b/\omega_0)q$.

One can see that for any $p, q \in -\infty, \infty$, the determination of the currents $\mathbf{I}_n^{(p,q)}$ from the system in Eq. (19), in which every equation is determined at the interval $t \in [0, T]$, was reduced to solving the system of equations with respect to a single vector $\mathbf{I}_n^{(0,0)}$, determined at different temporal intervals $(a/\omega_0)p + (b/\omega_0)q \leq t \leq T + (a/\omega_0)p + (b/\omega_0)q$. Since all these intervals are equal to the period of the fundamental frequency, it is sufficient to solve Equation (20) only at one of them defined, for example, by indices $p = q = 0$, i.e.,

$$\sum_{n=-\infty}^{\infty} \delta_n \mathbf{I}_n^{(0,0)} \exp\{jn\omega_0 t\} + \Re\left\{ \sum_{n=-\infty}^{\infty} \delta_n \tilde{\mathbf{Z}} (n\omega_0) \mathbf{I}_n^{(0,0)} \exp\{jn\omega_0 t\} + \mathbf{e}^{(0,0)} (t) \right\} = 0, \tag{21}$$

for any $t \in [0, T]$.

Thus, for the given properties of the LS matrix and system of excitation sources, the analysis of the circuit shown in Fig. 6(a) can be reduced to the analysis of the circuit shown in Fig. 6(b). This circuit consists of one nonlinear $2m$-pole described by the characteristic in Eq. (2a) and one linear multipole, whose impedance matrix is determined at the frequencies of all harmonics and equal to $\tilde{\mathbf{Z}}(n\omega_0)$ for any $n \in (-\infty, \infty)$. To analyze such a circuit, one should solve a system of the $m(2N + 1)$-th order equations (N is the number of retained current harmonics). Consequently, the solution of the state equations of the large rectenna in the infinite array approximation is reduced to solve the system of a single equivalent RRE as a part of an infinite array, whose circuit parameters are defined in this subsection. This allows us to develop an effective method for the rectenna calculation under equi-amplitude excitation by using available algorithms and software solutions for calculating only one RRE. This result is similar to the concept of a "single" cell known from the theory of linear antenna arrays [18].

2.4. External Parameters of the LRA

2.4.1. Description of the Linear Multipoles

As it was pointed out in Sec. 2.3.1, the linear multipoles at the stage of solving the state equations can be conveniently characterized by the matrices of intrinsic and mutual impedances. However, external parameters of the rectenna can be better described by using another approach. At this stage, the multipole LM-1, equivalent to the radiator system can be characterized by the scattering matrix $\mathbf{S}_R(\omega)$, column of the orthonormalized radiation patterns (RP), $\mathbf{e}(\omega, \theta, \varphi)$, column of partial RP, $\mathbf{g}(\omega, \theta, \varphi)$, and orthogonalizing matrix of incidental waves, i.e., to use the descriptions accepted in the matrix theory of antennas [19]. This is related to the fact that the external parameters of the rectenna for the radiator system can be characterized by the parameters defining its coupling with the external medium. Vectors $\mathbf{e}(\omega, \theta, \varphi)$ and $\mathbf{g}(\omega, \theta, \varphi)$ are just the required parameters.

Matrix $\mathbf{S}_R(\omega)$ connects the amplitudes of incidental $\mathbf{a}''(\omega)$ and reflected $\mathbf{b}''(\omega)$ waves at the inputs of the radiator system (the cross-section β-β, Fig. 7(a)) and the amplitudes of the convergent $\mathbf{u}'_d(\omega_0)$ and the divergent $\mathbf{u}'_d(\omega)$ spherical waves in the free space channels (cross-section δ-δ)

$$\begin{pmatrix} \mathbf{b}''(\omega) \\ \mathbf{u}'_d(\omega) \end{pmatrix} = \begin{pmatrix} \mathbf{S}_{\beta\beta} & \mathbf{S}_{\beta\delta} \\ \mathbf{S}_{\delta\beta} & \mathbf{S}_{\delta\delta} \end{pmatrix} \begin{pmatrix} \mathbf{a}''(\omega) \\ \mathbf{u}'_c(\omega_0) \end{pmatrix}. \tag{22}$$

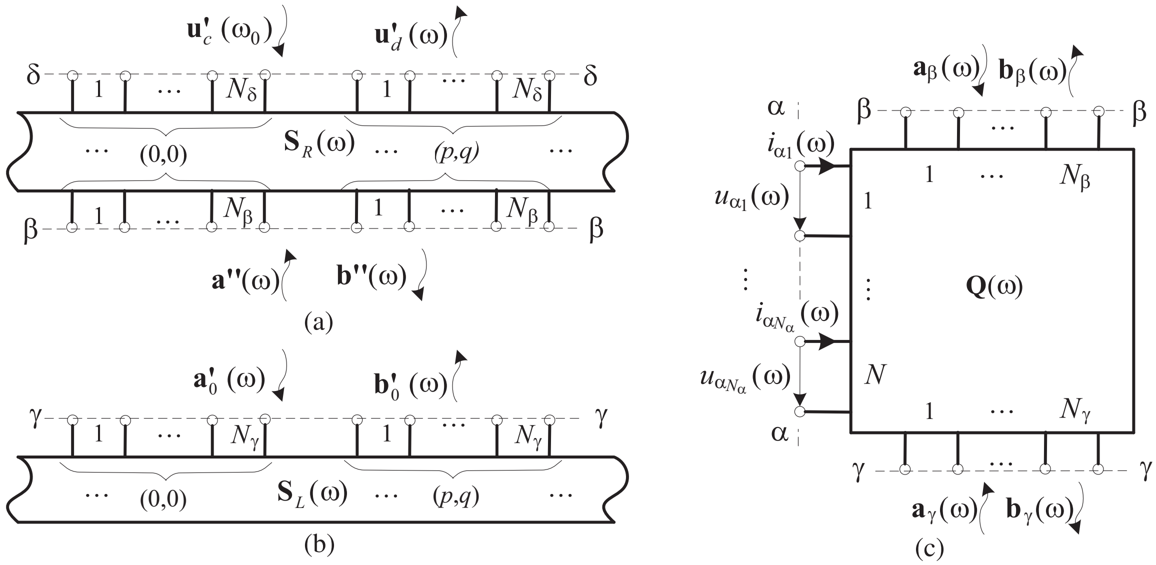

Figure 7. The representation of the linear rectenna subcircuits at the stage of the external parameter definition.

Vector $\mathbf{u}'_c(\omega_0)$ is related to the electric field intensity $\mathbf{E}(\omega_0,\theta,\varphi)$ of the exciting flat wave coming from the direction (θ,φ) in the following way

$$\mathbf{u'}_c(\omega_0) = -\frac{-j\lambda_0}{\sqrt{2W_0}}\mathbf{E}(\omega_0,\theta,\varphi)\mathbf{e}(\omega_0,\theta,\varphi) = -\frac{-j\lambda_0}{\sqrt{2W_0}}\mathbf{E}(\omega_0,\theta,\varphi)\mathbf{A}^T(\omega_0)\mathbf{g}(\omega_0,\theta,\varphi) \tag{23}$$

where W_0 is the wave impedance of the free space. In Equation (23), we take into account the relations between $\mathbf{e}(\omega_0,\theta,\varphi)$, $\mathbf{g}(\omega_0,\theta,\varphi)$ and $\mathbf{A}(\omega)$ which are determined by the relation proposed in [19]

$$\mathbf{e}(\omega,\theta,\varphi) = \mathbf{A}^T(\omega)\mathbf{g}(\omega,\theta,\varphi). \tag{24}$$

Multipole LM-2, which defines the energy receivers connected to the rectenna, is characterized by the scattering matrix $\mathbf{S}_L(\omega)$ relating complex amplitudes of the incident $\mathbf{a}'_0(\omega)$ and reflected $\mathbf{b}'_0(\omega)$ waves on its inputs (cross-section γ-γ, Fig. 7(b))

$$\mathbf{b}'_0(\omega) = \mathbf{S}_L(\omega)\,\mathbf{a}'_0(\omega)\,. \tag{25}$$

Let us define the linear multipole LM-3 by the mixed matrix $\mathbf{Q}(\omega)$, which relates (see Fig. 7(c)) the incidental and reflected waves in the cross-sections β-β and δ-δ to the normalized currents $\mathbf{i}_\alpha(\omega)$ and voltages $\mathbf{u}_\alpha(\omega)$ in the cross-section α-α, which connects LM-3 and the nonlinear multipole.

$$\begin{pmatrix} \mathbf{u}_\alpha(\omega) \\ \mathbf{b}_\beta(\omega) \\ \mathbf{b}_\gamma(\omega) \end{pmatrix} = \begin{pmatrix} \mathbf{Q}_{\alpha\alpha}(\omega) & \mathbf{Q}_{\alpha\beta}(\omega) & \mathbf{Q}_{\alpha\gamma}(\omega) \\ \mathbf{Q}_{\beta\alpha}(\omega) & \mathbf{Q}_{\beta\beta}(\omega) & \mathbf{Q}_{\beta\gamma}(\omega) \\ \mathbf{Q}_{\gamma\alpha}(\omega) & \mathbf{Q}_{\gamma\beta}(\omega) & \mathbf{Q}_{\gamma\gamma}(\omega) \end{pmatrix} \begin{pmatrix} \mathbf{i}_\alpha(\omega) \\ \mathbf{a}_\beta(\omega) \\ \mathbf{a}_\gamma(\omega) \end{pmatrix} \tag{26}$$

The blocks of matrix $\mathbf{Q}(\omega)$ can be calculated if the scattering matrix $\mathbf{S}(\omega)$ of the multipole LM-3 is known. This relation can be found in [15, 16].

The normalized currents $\mathbf{i}_\alpha(\omega)$ and voltages $\mathbf{u}_\alpha(\omega)$ are related to the complex voltage amplitudes $\mathbf{U}_\alpha(\omega)$ by the known relations

$$\begin{aligned} \mathbf{i}_\alpha(\omega) &= 0.5\,\{\mathbf{Z}_w\}^{1/2}\,\mathbf{I}_\alpha(\omega)\,, \\ \mathbf{u}_\alpha(\omega) &= 0.5\,\{\mathbf{Z}_w\}^{-1/2}\,\mathbf{U}_\alpha(\omega)\,, \end{aligned}$$

where $\{\mathbf{Z}_w\}^{1/2}$ and $\{\mathbf{Z}_w\}^{-1/2}$ are the diagonal matrixes with the elements defined as numbers $\sqrt{Z_{wl}(\omega)}$ (for $\{\mathbf{Z}_w\}^{1/2}$) and $1/\sqrt{Z_{wl}(\omega)}$ (for $\{\mathbf{Z}_w\}^{-1/2}$); $Z_{wl}(\omega)$ is the wave impedance at the frequency ω of the transmission line connected in the cross-section $\alpha\alpha$ to the l-th input of the nonlinear multipole. In what follows, we assume that the wave impedances of all lines are equal, i.e., $Z_{wl}(\omega) = Z_w(\omega)$ $(l = 1, \ldots, N_\alpha)$. Calculation of the external rectenna parameters requires that the following initial data should be given: the operating frequency ω_0, vector of the input stimuli $\mathbf{u}'_c(\omega_0)$, parameters of the multipoles included into the system, and complex current amplitudes $\mathbf{I}_n^{(p,q)}$, obtained by solving the state equations, which determine the normalized currents $\mathbf{i}_\alpha(\omega)$ at the frequency of the n-th harmonic in the cross-section α-α of all RRE arrays which are related as

$$\sqrt{Z_w}\mathbf{i}_\alpha(n\omega_0) = \left(\ldots, \mathbf{I}_n^{(-1,-q)}, \mathbf{I}_n^{(0,-q)}, \mathbf{I}_n^{(1,-q)}, \ldots, \mathbf{I}_n^{(-1,0)}, \mathbf{I}_n^{(0,0)}, \mathbf{I}_n^{(1,0)}, \ldots, \mathbf{I}_n^{(-1,q)}, \mathbf{I}_n^{(0,q)}, \mathbf{I}_n^{(1,q)}, \ldots\right)^T. \quad (27)$$

2.4.2. Rectenna Parameters

The external parameters of the rectenna at frequency ω can be derived by determining the vectors $\mathbf{a}'_0(\omega)$ and $\mathbf{u}'_d(\omega)$ for the given input stimuli $\mathbf{u}'_c(\omega_0)$ and the known vector $\mathbf{i}_\alpha(\omega)$ found as solution of the state equations. In what follows, ω stands for any frequency $n\omega_0$ for $n = 0, 1, \ldots$ if further clarification is not necessary. The parameters of a linear subcircuit will be presented by the mixed matrix $\mathbf{Q}^A(\omega)$ whose definition and relations for calculating its blocks using the parameters LM-1, LM-2 and LM-3 are given in [15, 16]. Relations, which describe the relationship between vectors $\mathbf{a}'_0(\omega)$, $\mathbf{u}'_d(\omega)$ and vectors $\mathbf{u}'_c(\omega_0)$, $\mathbf{i}_\alpha(\omega)$, can be written as follows

$$\mathbf{a}'_0(\omega) = \mathbf{Q}^A_{\gamma\alpha}(\omega)\mathbf{i}_\alpha(\omega_0) + \begin{cases} \mathbf{Q}^A_{\gamma\delta}(\omega_0)\mathbf{u}'_c(\omega_0) & \text{if} \quad \omega = \omega_0 \\ 0 & \text{if} \quad \omega \neq \omega_0 \end{cases}, \quad (28)$$

$$\mathbf{u}'_d(\omega) = \tilde{\mathbf{Q}}_{\delta\alpha}(\omega)\mathbf{i}_\alpha(\omega_0) + \begin{cases} \tilde{\mathbf{Q}}_{\delta\delta}(\omega_0)\mathbf{u}'_c(\omega_0) & \text{if} \quad \omega = \omega_0 \\ 0 & \text{if} \quad \omega \neq \omega_0 \end{cases}. \quad (29)$$

The obtained expressions represent a system of output equations describing the reactions of the generalized rectenna circuit (Fig. 2), in the cross-sections γ-γ and δ-δ where NM is represented by the equivalent current sources $\mathbf{i}_\alpha(\omega)$. The currents are determined by solving the state equations using external stimuli $\mathbf{u}'_c(\omega_0)$.

Relations (28) and (29) are formally defined as linear relations, connecting the vector of input parameters and vectors $\mathbf{u}'_c(\omega_0)$ and $\mathbf{i}_\alpha(\omega)$. However, the nonlinear dependency of $\mathbf{i}_\alpha(\omega)$ upon $\mathbf{u}'_c(\omega_0)$, described by the state equations, results in a nonlinear dependency of the input parameters $\{\mathbf{a}'_0(\omega), \mathbf{u}'_d(\omega)\}^T$ on the input stimuli $\mathbf{u}'_c(\omega_0)$. This results in a nonlinear dependency of all the external rectenna parameters on the input stimuli. Therefore, if the rectenna should be characterized by some input parameters, it is necessary to specify a level of input stimuli for which the given level is obtained. In addition, the nonlinear rectifier diodes give rise to new spectral components in the current spectrum $\mathbf{i}_\alpha(\omega)$ at the inputs (α-α) of the linear subcircuit whose frequencies ω differ from the frequencies of input stimuli ω_0. At these frequencies $\mathbf{u}'_c(\omega \neq \omega_0) \equiv 0$, therefore relations (28) and (29) can be simplified

$$\mathbf{a}'_0(\omega) = \mathbf{Q}^A_{\gamma\alpha}(\omega)\mathbf{i}_\alpha(\omega_0), \quad (30)$$

$$\mathbf{u}'_d(\omega) = \tilde{\mathbf{Q}}_{\delta\alpha}(\omega)\mathbf{i}_\alpha(\omega_0). \quad (31)$$

Let us determine the external key parameters of the rectenna: the DC voltages and currents in the load, DC power absorbed by the multipole load, rectenna COP, and field reradiated by the rectenna at the fundamental frequency and its upper harmonics. The parameters are calculated in the following way.

We assume that the DC connections between RREs within the boundaries of the rectenna aperture are of the same type. Based on this assumption, we can determine the DC current and voltage at the array load. For the series collection scheme, we have

$$U_0 = N_0 U_{0RRE}, \quad I_0 = I_{0RRE}. \quad (32)$$

The voltage and current for the parallel collection scheme are related as

$$U_0 = U_{0RRE}, \quad I_0 = N_0 I_{0RRE}. \quad (33)$$

Here U_{0RRE}, I_{0RRE} are the voltage and current in a load of a single RRE; U_0, I_0 are the voltage and current in the load of the rectenna when the number of RREs is N_0.

The collection scheme of same type (either parallel or series) under an equi-amplitude excitation of the large rectenna is optimal in a sense that the COP of this collection schemes is equal to one under a condition that the loads of the RRE are equal at the main frequency and its upper harmonics. This fact follows from identity of the characteristics of all the rectenna RREs as sources of DC voltage. At the same time, the load impedances, which are required to achieve the maximum, COP of the RRE and, hence, the maximal COP of the rectenna for the series and parallel collection schemes can be different. Options for the optimal collection schemes are not limited by the only one type of RRE connections. For example, all the serial and parallel circuits of a hierarchical type, which at any hierarchy level has the same number of combined elements (parallel or series) will also have the COP equal to one [20].

The DC power absorbed in the multipole load can be calculated as

$$P_0 = \mathbf{a}_0'^{*T}(\omega)(\mathbf{E} - \mathbf{S}_L^{*T}(\omega)\mathbf{S}_L(\omega))\,\mathbf{a}_0'(\omega)\big|_{\omega\to 0}\,. \tag{34}$$

Here vector $\mathbf{a}_0'(\omega)|_{\omega\to 0}$ is defined from Equation (30), $\mathbf{a}_0'(\omega)|_{\omega\to 0} = \mathbf{Q}_{\gamma\alpha}^{A}(n\omega_0)\mathbf{i}_\alpha(n\omega_0)|_{n=0}$, and $\mathbf{E}$ is the unit matrix.

The rectenna COP is defined as the ratio between power P_0 and maximal power P_M that can be harvested from the incident field by the radiator system if the load is optimal

$$\eta = \frac{P_0}{P_M} = \frac{P_0}{\mathbf{u}_c'^{*T}(\omega_0)\mathbf{u}_c'(\omega_0)} = \frac{2W_0P_0}{\lambda_0^2|\mathbf{E}|^2\mathbf{g}^{*T}(\omega_0,\theta,\varphi)\mathbf{A}^*(\omega_0)\mathbf{A}^T(\omega_0)\mathbf{g}(\omega_0,\theta,\varphi)} \tag{35}$$

When the rectenna is excited by an electromagnetic wave with a frequency ω_0, the secondary field $\mathbf{E}_S$ is formed in the surrounding space. The scattered field in the wave zone at the fundamental frequency can be represented by two terms [19]

$$\begin{aligned}\mathbf{E}_S\left(\omega_0,\theta,\varphi\right) &= \mathbf{E}_\Sigma\left(\omega_0,\theta,\varphi\right) + \mathbf{E}_C\left(\omega_0,\theta,\varphi\right)\\ &= \sqrt{2W_0}\mathbf{a}''^T\left(\omega_0\right)\mathbf{g}\left(\omega_0,\theta,\varphi\right)\frac{\exp\left(-jk_0r\right)}{r} + \mathbf{E}_C\left(\omega_0,\theta,\varphi\right),\end{aligned} \tag{36}$$

where $\mathbf{E}_\Sigma(\omega_0,\theta,\varphi)$ is the secondary field initiated by the current flow at the terminals of the rectenna radiators, and $\mathbf{E}_C(\omega_0,\theta,\varphi)$ is the field scattered by the matched radiators and design elements, $\mathbf{a}''(\omega_0)$ if the incident wave at the inputs of rectenna radiators is defined as

$$\mathbf{a}''\left(\omega\right) = \left(\mathbf{E} - \mathbf{S}_{\beta\beta}\tilde{\mathbf{Q}}_{\beta\beta}\right)^{-1}\left(\mathbf{S}_{\beta\beta}\tilde{\mathbf{Q}}_{\beta\alpha}\mathbf{i}_\alpha\left(\omega\right) + \begin{cases}\mathbf{S}_{\beta\gamma}\mathbf{u}_c'\left(\omega_0\right) & \text{if} \quad \omega = \omega_0\\ 0 & \text{if} \quad \omega \neq \omega_0\end{cases}\right). \tag{37}$$

The matrices $\tilde{\mathbf{Q}}_{ij}$ are computed by using the parameters of the linear multiport as

$$\tilde{\mathbf{Q}}_{ij} = \mathbf{Q}_{ij} + \mathbf{Q}_{i\gamma}\left(\mathbf{E} - \mathbf{S}_L\mathbf{Q}_{\gamma\gamma}\right)^{-1}\mathbf{S}_L\mathbf{Q}_{\gamma j}, \quad i = \alpha,\beta; \quad j = \alpha,\beta. \tag{38}$$

At the frequencies of upper harmonics, the radiators of the rectenna are excited from the side of the input terminals. Therefore, the scattering field at the frequencies $\omega_n = n\omega_0$ has only one component, $\mathbf{E}_\Sigma(\omega_n,\theta,\varphi)$. The scattered field in the far zone at the fundamental frequency and its upper harmonics is determined by the expression [19]

$$\mathbf{E}_S(\omega_n,\theta,\varphi) = \sqrt{2W_0}\mathbf{a}''^T\left(\omega_n\right)\mathbf{g}\left(\omega_n,\theta,\varphi\right)\frac{\exp\left(-jnk_0r\right)}{r}. \tag{39}$$

Since all RRE parameters under equiamplitude excitation are identical, formula (39) can be represented as follows

$$\mathbf{E}_S\left(\omega_n,\theta,\varphi\right) = \sqrt{2W_0}\mathbf{a}_0''^T\left(\omega_n\right)\mathbf{g}_0\left(\omega_n,\theta,\varphi\right)F\left(\omega_n,\theta,\varphi\right)\frac{\exp\left(-jnk_0r\right)}{r}, \tag{40}$$

where $\mathbf{a}''_{0t}(\omega_n)$ and $\mathbf{g}_0(\omega_n,\theta,\varphi)$ are the amplitude of the incidental waves and the partial RP of the RREs radiator at the frequency of the n-th harmonic, and $F(\omega_n,\theta,\varphi)$ is the array multiplier at the same frequency.

If the parameters of the RRE radiators are defined, the field $\mathbf{E}_S(\omega_n,\theta,\varphi)$ can be easily calculated.

3. MODEL VERIFICATION

As shown in Subsection 2.3.3, the nonlinear mode of the LRA excited by periodic fields can be studied by examining the mode of one equivalent RRE operating in the infinite array. This approach has allowed us to develop the effective algorithm for simulation of electrodynamic and energy characteristic of the rectenna structures and DC power collection circuits which take into account nonlinear effects. A software package for simulation of the rectenna system whose radiating structure is a periodic planar array of microstrip radiators with arbitrary geometry was implemented based on the proposed method

To determine the reliability of the developed technique, the rectenna experiments were performed by wireless energy transmission using microwave beams. The transmitting equipment of the WPT system consisted of a microwave generator, which was placed outside the anechoic chamber, and a mirror antenna. The generator was working at 2.45 GHz.

The rectenna developed for the model verification consists of nine single-type modules (Fig. 8(a)). The design of these base module with dimensions of 0.7 m × 0.7 m allowed us to easily increase the rectenna aperture. Fig. 8(b) shows a schematic diagram of the base module, which consists of 16 RREs (eight parallel strips with the RRE tandem). The module elements were placed at the nodes of a triangular grid with spacing equal to $\lambda/2$.

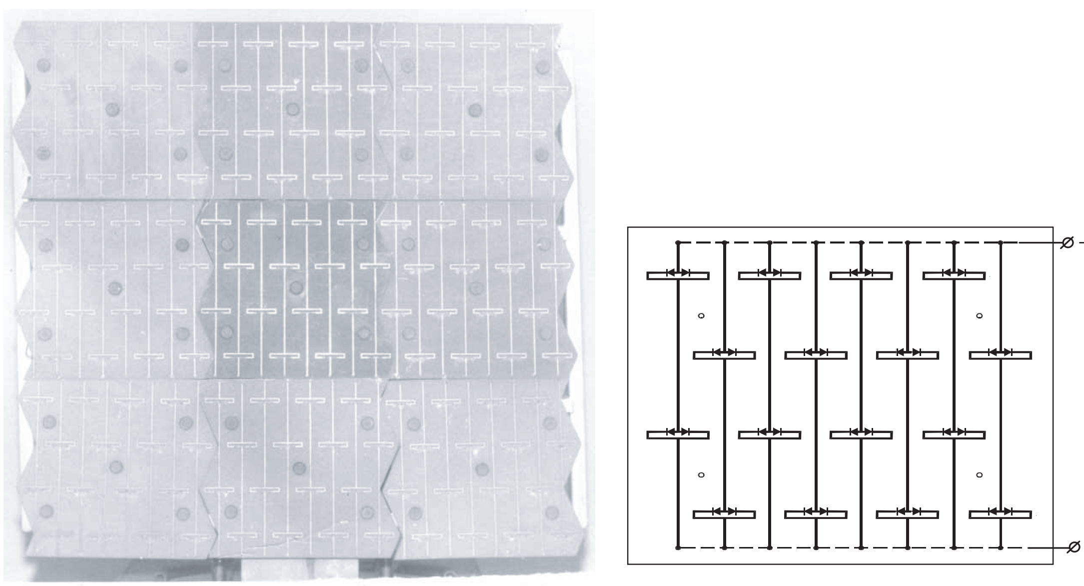

(a) (b)

Figure 8. The experimental rectenna: (a) design; (b) the schematic diagram of the base module.

Loop vibrators over a screen were used as antennas; two opposite connected diodes 3A208A with power-carrying capacity of 0.5 watts were connected to each vibrator. The vibrators were resonantly tuned taking into account the diodes capacitance. Decoupling between the rectifier and DC circuits in the RRE was carried out by connecting the wires of the power collection circuit to the point of zero potential of the loop vibrator. The printed-circuit board of the module foil-clad was made of a glass fiber laminate ($\varepsilon_r = 6$) whose thickness was 2 mm, placed at a height of 9 mm over the screen. The rectenna consisted of 144 RREs.

The rectenna was designed so that the modules can be DC interconnected in series, parallel or series-parallel. A separate load resistor can be connected to each module.

The experimental and simulated results are presented in Fig. 9, where the DC power (Fig. 9(a)) and voltage (Fig. 9(b)) are plotted versus load resistance. The experimental and simulated results are marked by circles and solid lines, respectively. For the optimal load resistance $R_{Lopt} = 120\,\text{Ohm}$, obtained from Fig. 9(a), the rectification COP was also measured and equals 87.9%. The relative measurement error was $\Delta_m \pm 19.5\%$.

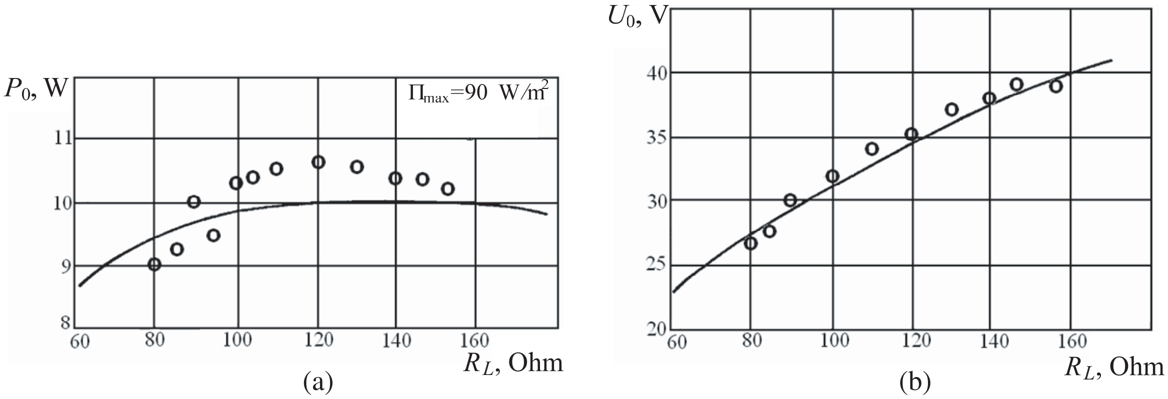

Figure 9. The DC power and voltage versus the load resistance for the experimental rectenna: (a) power; (b) voltage; Π_{max} is power flux density at the rectenna. The energy transmission was performed at the distance of 3 m.

Analysis of the simulated and experimental results has proved the possibility to design large rectennas using the infinite periodic array approximation and applicability of the theoretical rectenna models and the corresponding software package.

4. CONCLUSION

The mathematical model of the LRA exited by the periodic field has been developed. The model is based on a generalized antenna model containing nonlinear elements. The advantage of the rectenna mathematical model consists in that the computation of the multielement rectenna array can be reduced to calculation of the single equivalent element of the rectenna. This significantly reduces the modeling time. The proposed mathematical model allows us to take into account all parameters of the linear and nonlinear elements included into the rectenna. The model can be used for effective development of the rectennas with predetermined characteristics, by using spatialized software or commercial packages containing modules for electrodynamic and circuit simulation (e.g., AWR, ADS, ANSYS Electronics Desktop). The LRA model was verified by comparison of the simulated and experimental results. It should be mentioned that strict requirements should be imposed on size and weight characteristics of the rectenna. Therefore, it makes sense to use impedance vibrators, which can reduce the size of the rectennas [21–26].

REFERENCES

1. Mankins, Y. C., "A technical overview of the "sun tower" solar power satellite concept," *Acta Astronavtica*, Vol. 50, 369–377, 2002.
2. Masumoto, H., "Research on solar power satellites and microwave power transmission in Japan," *IEEE Microwave Magazine*, Vol. 3, 36–45, 2002.
3. Hashimoto, K. and N. Shinohara, "Solar power satellite and its EMC issues," *EMC'09*, 29–32, Kyoto, 2009.
4. Shinohara, N., "Beam control technologies with a high efficiency phased array for microwave power transmission in Japan," *Proceedings of the IEEE*, Vol. 101, 1448–1463, 2013.
5. Celeste, A., P. Jeanty, and G. Pignolet, "Case study in Reunion Island," *Acta Astronautica*, Vol. 54, 253–258, 2004.
6. Gomozov, A. V., D. V. Gretskih, V. M. Shokalo, and Sh. F. A. Al-Sammarraie, "Principles of construction and application of the microwave systems for wireless energy transmission of ground and space basing," *IEEE Computational Problems of Electrical Engineering*, Vol. 2, 15–23, 2012.

7. Dickinson, R. M., "Power in the sky: Requirements for microwave wireless power beamers for powering high-altitude platforms," *IEEE Microwave Magazine*, Vol. 14, 36–47, 2013.
8. Wu, Y., J. Linnartz, et al., "Modeling of RF energy scavenging for batteryless wireless sensors with low input power personal indoor and mobile radio communications," *PIMRC, IEEE 24th International Symposium*, 527–531, 2013.
9. Lu, X., P. Wang, D. Niyato, et al., "Wireless networks with RF energy harvesting: A contemporary survey," *IEEE Communications Surveys and Tutorials*, Vol. 17, 757–789, 2015.
10. Kotter, D. K., S. D. Novack, W. D. Slafer, and P. J. Pinhero, "Theory and manufacturing processes of solar nanoantenna electromagnetic collectors," *Journal of Solar Energy Engineering-transactions of the Asme*, Vol. 132, 2010, http://www.academia.edu/8220294.
11. Bankov, S. E., "Signal detection in a radiating nonlinear electromagnetic crystal," *Journal of Radio Electronics*, No. 1, 2012, http://jre.cplire.ru/jre/jan12/1/text.pdf (in Russian).
12. Semenikhina, D. V., A. I. Semenikhin, T. Y. Privalova, and V. V. Demshevsky, "Parametrical excitation microstrip lattice with nonlinear loads," *International Conference on Electromagnetics in Advanced Applications (ICEAA)*, 245–248, 2014.
13. Huang, W., B. Zhang, X. Chen, K. Huang, and C. Liu, "Study on an S-band rectenna array for wireless microwave power transmission," *Progress In Electromagnetics Research*, Vol. 135, 747–758, 2013.
14. Matsunaga, T., E. Nishiyama, and I. Toyoda, "5.8-GHz stacked differential rectenna suitable for large-scale rectenna arrays with DC connection," *IEEE Trans. Antennas and Propag.*, Vol. 63, 5944–5949, 2015.
15. Shifrin, Ya. S. and A. I. Luchaninov, "Antennas with nonlinear elements," *The Reference Manual on Antenna Equipment*, Vol. 1, 207–235, Moscow, 1997 (in Russian).
16. Luchaninov, A. I. and Y. S. Shifrin, "Mathematical model of antenna with lumped nonlinear elements," *Telecommunications and Radio Engineering*, Vol. 66, No. 9, 763–803, 2007.
17. Shifrin, Y. S., A. I. Luchaninov, and A. S. Posokhov, "Structural model of antennas with nonlinear elements," *Telecommunications and Radio Engineering*, Vol. 59, Nos. 1–2, 32–48, 2003.
18. Amitay, N., V. Galindo, and C. P. Wu, *Theory and Analysis of Phased Array Antennas*, John Wiley & Sons Inc, New York, 1972.
19. Sazonov, D. M., *Multi-element Antenna Systems*, Matrix Approach, Publishing House "Radiotekhnika", Moscow, 2015 (in Russian).
20. Shokalo, M. V., A. I. Luchaninov, A. M. Rybalro, and D. V. Gretskih, "Large-aperture rectifying antennas for wireless energy transfer by a microwave beam," Kollegium, Kharkov, 2006 (in Russian).
21. Nesterenko, M. V., V. A. Katrich, and V. M. Dakhov, "Formation of the radiation field with the set spatial-polarization characteristics by the crossed impedance vibrators system," *Radiophysics and Quantum Electronics*, Vol. 53, 371–378, 2010.
22. Nesterenko, M. V., V. A. Katrich, Y. M. Penkin, V. M. Dakhov, and S. L. Berdnik, *Thin Impedance Vibrators. Theory and Applications*, Springer Science+Business Media, New York, 2011.
23. Nesterenko, M. V., V. A. Katrich, V. M. Dakhov, and S. L. Berdnik, "Impedance vibrator with arbitrary point of excitation," *Progress In Electromagnetics Research B*, Vol. 5, 275–290, 2008.
24. Nesterenko, M. V., "Analytical methods in the theory of thin impedance vibrators," *Progress In Electromagnetics Research B*, Vol. 21, 299–328, 2010.
25. Nesterenko, M. V., V. A. Katrich, S. L. Berdnik, Y. M. Penkin, and V. M. Dakhov, "Application of the generalized method of induced EMF for investigation of characteristics of thin impedance vibrators," *Progress In Electromagnetics Research B*, Vol. 26, 149–178, 2010.
26. Penkin, Yu. M., V. A. Katrich, and M. V. Nesterenko, "Development of fundamental theory of thin impedance vibrators," *Progress In Electromagnetics Research M*, Vol. 45, 185–193, 2016.